Acta Mathematica Scientia, 2023, **43B**(3): 1439–1461
https://doi.org/10.1007/s10473-023-0325-y

Acta Mathematica Scientia 数学物理学报
http://actams.apm.ac.cn

FIXED/PREASSIGNED-TIME SYNCHRONIZATION OF QUATERNION-VALUED NEURAL NETWORKS INVOLVING DELAYS AND DISCONTINUOUS ACTIVATIONS: A DIRECT APPROACH*

Wanlu WEI (魏琬璐) *Cheng HU* (胡成)† *Juan YU* (于娟) *Haijun JIANG* (蒋海军)
College of Mathematics and System Science, Xinjiang University, Urumqi 830017, China
E-mail: *wwl15744@163.com; hucheng@xju.edu.cn; yujuanseesea@163.com; jianghai@xju.edu.cn*

Abstract The fixed-time synchronization and preassigned-time synchronization are investigated for a class of quaternion-valued neural networks with time-varying delays and discontinuous activation functions. Unlike previous efforts that employed separation analysis and the real-valued control design, based on the quaternion-valued signum function and several related properties, a direct analytical method is proposed here and the quaternion-valued controllers are designed in order to discuss the fixed-time synchronization for the relevant quaternion-valued neural networks. In addition, the preassigned-time synchronization is investigated based on a quaternion-valued control design, where the synchronization time is preassigned and the control gains are finite. Compared with existing results, the direct method without separation developed in this article is beneficial in terms of simplifying theoretical analysis, and the proposed quaternion-valued control schemes are simpler and more effective than the traditional design, which adds four real-valued controllers. Finally, two numerical examples are given in order to support the theoretical results.

Key words fixed-time synchronization; preassigned-time synchronization; quaternion-valued neural networks; discontinuous activation; direct analysis method

2010 MR Subject Classification 93B52; 93C23

1 Introduction

Quaternion-valued neural networks (QVNNs) were proposed in 1995 for the study of color image recognition [1], in which the state of each neuron is represented by a quaternion. One of the strengths of QVNNs is that they can express 3-D affine transformations efficiently and compactly. In addition, QVNNs have significant advantages over real-valued neural networks (RVNNs) and complex-valued neural networks (CVNNs) when dealing with high-dimensional

*Received February 4, 2022; revised August 25, 2022. This work was supported by the National Natural Science Foundation of China (61963033, 61866036, 62163035), the Key Project of Natural Science Foundation of Xinjiang (2021D01D10), the Xinjiang Key Laboratory of Applied Mathematics (XJDX1401) and the Special Project for Local Science and Technology Development Guided by the Central Government (ZYYD2022A05).
†Corresponding author

data [2–4]. However, because of the incommutability of quaternion multiplication, the progress of research on QVNNs was held back for many years. Recently, however research on QVNNs has become increasingly abundant, due to the improvement of quaternion theory and the associated research analysis methods. By decomposing QVNNs into two complex-valued systems, several sufficient conditions were established in [5–7] to achieve global μ-stability. By decomposing QVNNs models into four real-valued systems, several sufficient criteria to ensure exponential stability were derived in [8–10].

In addition to dynamics analysis, in view of the potential applications in secure communication and image encryption, research on the synchronization control of QVNNs has begun to attract the attention of more and more scholars. Actually, synchronization is a significant dynamic phenomenon in chaotic neural networks, and this has important applications in fields such as information processing [11] and secure communication [12]. Many synchronization results about QVNNs have been published, including global asymptotic synchronization [13, 14], exponential synchronization [15, 16], and finite-time (FNT) synchronization [17]. As opposed to asymptotic or exponential synchronization, it is allowed in FNT synchronization to achieve synchronization in a finite time, and has the advantages of faster convergence and stronger anti-interference. However, the settling time (ST) of FNT synchronization relies on the initial states, which indicates that it is extremely difficult to discuss FNT synchronization for systems with unknown initial values. To overcome this shortcoming, fixed-time (FXT) control and synchronization were proposed [18, 19], here the estimate of the ST was improved to become independent of the initial values. So far, the FXT synchronization of RVNNs and CVNNs has been extensively studied [20–25], but the related results on QVNNs are relatively few. In [26, 27], the FXT synchronization of QVNNs was discussed by a separation method and by designing nonlinear control schemes. Based on the separation technique, the FXT synchronization for a class of QVNNs without delay was discussed in [28], this was achieved by designing pure power law control strategies. By proposing nonlinear and delayed feedback controllers for the separated real-valued submodels in [29, 30], FNT synchronization and FXT synchronization were investigated for memristor-based QVNNs with time delays. The authors of [31] studied FNT and FXT anti-synchronization of QVNNs with inconsistent Markovian and reaction-diffusion terms by designing discontinuous control laws for the separated real-valued systems.

Note that the FXT synchronization in [26–31] was analyzed based on the separation method, which greatly increases the redundancy of the theoretical calculations. In addition, FXT synchronization was achieved by adding four real-valued controllers, which not only increases the cost of control, but also reduces the feasibility of control strategies. Therefore, it is a natural idea to directly design quaternion-valued control schemes for analyzing the FXT synchronization of QVNNs. Inspired by the complex-valued sign functions proposed in [20], Li *et al.* proposed the quaternion-valued sign function in [32], and discussed the FNT anti-synchronization of QVNNs with continuous activation functions based on the non-separation method. Subsequently, Peng *et al.* studied the FNT synchronization and FXT synchronization of QVNNs with continuous activation functions based on the non-separation method by designing quaternion-valued controllers in [33] and by switching control strategies in [34]. However, it is noted that neural networks with discontinuous activation functions are ideal models for describing nonlinear

physical problems with high slopes [35]. Furthermore, it has been shown that neural networks composed of discontinuous activation functions can deal perfectly with dry friction problems, optimization problems, and switching problems in electronic circuits [36]. Thus, the study of neural networks with discontinuous activation functions has great theoretical value and practical significance.

In addition to FXT synchronization, preassigned-time (PAT) synchronization has been a hot topic in recent years. Differently from FNT synchronization and FXT synchronization, the convergence time of PAT synchronization is preappointed based on practical and specific needs that are independent of the initial states and model parameters [37]. Although synchronization may also be realized for an appointed time by adjusting control parameters in FXT synchronization controllers, this approach is not the best choice because the relationship between the convergence time and control parameters is unclear, and the adjustment is blind and time-consuming. Therefore, it is of great significance to study PAT synchronization by designing feasible control laws for a specified convergence time. At present, there are many research results on FNT control [38] and FXT control [39], but the PAT synchronization of complex systems needs to be further explored [40–42]. In [28], by introducing four real-valued controllers, the PAT synchronization problem of a class of QVNNs without delay was considered by the separation method. As pointed out in the above discussion, the separation analysis undoubtedly results in a large amount of calculation, a high control cost and low feasibility in terms of practical applications. It would be valuable to develop a direct analysis technique to investigate the PAT synchronization of QVNNs.

This article aims to develop a direct analysis method and propose quaternion-valued control schemes to discuss the FXT and PAT synchronization of QVNNs with time-varying delays and discontinuous activation functions. The most innovative elements of this work are as follows.

(1) Differently from QVNN models with continuous activations in [33, 34], a class of QVNNs involving discontinuous activation functions is here considered and several important properties of the quaternion-valued signum function are established in order to effectively deal with the QVNN model in the quaternion field.

(2) Based on the quaternion-valued signum function and the established properties, a direct analytical method without separation is proposed and quaternion-valued discontinuous control schemes are developed in order to investigate FXT synchronization of QVNNs. Compared with the separation method and real-valued design in [26–31], the direct approach developed here greatly reduces the amount of calculation needed in the theoretical analysis and improves the feasibility of control strategies in applications.

(3) In addition to FXT synchronization, PAT synchronization for QVNNs is investigated by designing discontinuous quaternion-valued control laws, where the synchronization time is prespecified and is independent of the initial states and model parameters. Note that the control scheme here is implemented in the quaternion field, which is more feasible and effective in comparison with the separation-based real-valued design in [28].

The rest of this article is organized as follows: Some basic preparations and research models are provided in Section 2. The FXT synchronization and PAT synchronization for QVNNs are studied in Sections 3 and 4. In Section 5, two numerical examples are given to verify the theoretical results. Finally, a brief summary of this paper is given in Section 6.

Notations In this article, $\vec{n} = \{1, 2, \cdots, n\}$, $\mathbb{R}^n$ is a space consisting of n-dimensional real vectors and $\mathbb{H}^n$ is a space composed of all n-dimensional quaternion vectors. 0_n denotes an n-dimensional vector where all the entries are zero. $\mathfrak{F} = C([-\tau, 0], \mathbb{H}^n)$ is a set composed of all continuous functions on $[-\tau, 0]$. The 1-norm and the 2-norm of a are defined as $\|a\|_1 = |a^R| + |a^I| + |a^J| + |a^K|$ and $\|a\|_2 = \sqrt{a\bar{a}}$, respectively, where $\bar{a} = a^R - a^I i - a^J j - a^K k$ represents the conjugate of a. Denote that $d = R, I, J, K$, and for a discontinuous function f, let $f^{d-}(x)$ and $f^{d+}(x)$ be the left and right limits of the real or imaginary parts of f at x, and let $\check{f}^d(x)$ and $\hat{f}^d(x)$ be the minimum and the maximum between $f^{d-}(x)$ and $f^{d+}(x)$. Define the convex hull as $\overline{\text{co}}[f(x)] = \overline{\text{co}}[f^R(x)] + \overline{\text{co}}[f^I(x)]i + \overline{\text{co}}[f^J(x)]j + \overline{\text{co}}[f^K(x)]k = [\check{f}^R(x), \hat{f}^R(x)] + [\check{f}^I(x), \hat{f}^I(x)]i + [\check{f}^J(x), \hat{f}^J(x)]j + [\check{f}^K(x), \hat{f}^K(x)]k$.

2 Preliminaries and Model Description

Consider the following QVNN model consisting of n neurons and involving time-varying delays:

$$\dot{x}_p(t) = -\xi_p x_p(t) + \sum_{q=1}^{n} a_{pq} f_q(x_q(t)) + \sum_{q=1}^{n} b_{pq} g_q(x_q(t - \tau_{pq}(t))) + I_p(t), \quad p \in \vec{n}. \tag{2.1}$$

Here $x_p \in \mathbb{H}$ is the state of the p-th neuron, $\xi_p \in \mathbb{H}$ is the feedback self-connection weight, $f_q(\cdot)$ and $g_q(\cdot) : \mathbb{H} \to \mathbb{H}$ are discontinuous quaternion activation functions without and with time delays. a_{pq}, $b_{pq} \in \mathbb{H}$ denote the connection weights of the qth neuron on the pth neuron at t and $t - \tau_{pq}(t)$, $\tau_{pq}(t)$ is the time-varying delay satisfying $0 \le \tau_{pq}(t) \le \tau$, while $I_p(t) \in \mathbb{H}$ is the external input function. The initial condition of system (2.1) is provided by

$$x_p(s) = \sigma_p(s), \quad s \in [-\tau, 0], \quad p \in \vec{n},$$

and $\sigma(s) = (\sigma_1(s), \cdots, \sigma_n(s))^T \in \mathfrak{F}$.

Let model (2.1) be the master model. The slave model is given as

$$\dot{y}_p(t) = -\xi_p y_p(t) + \sum_{q=1}^{n} a_{pq} f_q(y_q(t)) + \sum_{q=1}^{n} b_{pq} g_q(y_q(t - \tau_{pq}(t))) + I_p(t) + u_p(t), \quad p \in \vec{n}, \tag{2.2}$$

where $y_p \in \mathbb{H}$ denotes the state variable of the slave model, $u_p(t) \in \mathbb{H}$ is the external controller and will be developed later, and other parameters are defined as in model (2.1). The initial condition of system (2.2) is provided by

$$y_p(s) = \tilde{\sigma}_p(s), \quad s \in [-\tau, 0], \quad p \in \vec{n},$$

and $\tilde{\sigma}(s) = (\tilde{\sigma}_1(s), \cdots, \tilde{\sigma}_n(s))^T \in \mathfrak{F}$.

Assumption 1 ([19]) For $q \in \vec{n}$, f_q and g_q are continuous except on countable sets of isolated points $\{u_r^q\}$ and $\{v_r^q\}$, respectively, and $f_q^{d-}(u_r^q)$, $f_q^{d+}(u_r^q)$ and $g_q^{d-}(v_r^q)$, $g_q^{d+}(v_r^q)$ exist. Moreover, in every bounded compact interval, there are a finite number of jump points at most for f_q and g_q.

Definition 2.1 ([20]) A continuous function vector $x(t) = (x_1(t), \cdots, x_n(t))^T : [-\tau, T_0) \to \mathbb{H}^n$ is called a solution of system (2.1) on $[-\tau, T_0)$ if

(1) x is absolutely continuous on $[0, T_0)$;

(2) there exist measurable functions $\alpha = (\alpha_1, \cdots, \alpha_n)^T : [0, T_0) \to \mathbb{H}^n$ and $\tilde{\alpha} = (\tilde{\alpha}_1, \cdots, \tilde{\alpha}_n)^T : [-\tau, T_0) \to \mathbb{H}^n$ satisfying $\alpha_q \in \overline{\text{co}}[f_q(x_q)]$, $\tilde{\alpha}_q \in \overline{\text{co}}[g_q(x_q)]$ such that

$$\dot{x}_p(t) = -\xi_p x_p(t) + \sum_{q=1}^{n} a_{pq}\alpha_q(t) + \sum_{q=1}^{n} b_{pq}\tilde{\alpha}_q(t - \tau_{pq}(t)) + I_p(t), \quad p \in \vec{n} \tag{2.3}$$

for almost everywhere (a.e.) $t \in [0, T_0)$.

Similarly, for slave model (2.2), there exist measurable functions $\beta_q \in \overline{\text{co}}[f_q(y_q)]$ and $\tilde{\beta}_q \in \overline{\text{co}}[g_q(y_q)]$ such that

$$\dot{y}_p(t) = -\xi_p y_p(t) + \sum_{q=1}^{n} a_{pq}\beta_q(t) + \sum_{q=1}^{n} b_{pq}\tilde{\beta}_q(t - \tau_{pq}(t)) + I_p(t) + u_p(t), \quad p \in \vec{n} \tag{2.4}$$

for a.e. $t \in [0, T_0)$.

Denoting that $e_p(t) = y_p(t) - x_p(t)$ with $p \in \vec{n}$, from (2.3) and (2.4), the following error system is derived

$$\begin{aligned} \dot{e}_p(t) = &- \xi_p e_p(t) + \sum_{q=1}^{n} a_{pq}\big(\beta_q(t) - \alpha_q(t)\big) \\ &+ \sum_{q=1}^{n} b_{pq}\Big(\tilde{\beta}_q\big(t - \tau_{pq}(t)\big) - \tilde{\alpha}_q\big(t - \tau_{pq}(t)\big)\Big) + u_p(t), \quad p \in \vec{n}. \end{aligned} \tag{2.5}$$

Definition 2.2 ([40]) QVNNs (2.1) and (2.2) are said to be FXT synchronized if there exists a time point $0 < T < +\infty$ which is related to the system parameters, for any solutions of (2.1) and (2.2) denoted by

$$x(t) = \big(x_1(t), x_2(t), \cdots, x_n(t)\big)^T \quad \text{and} \quad y(t) = \big(y_1(t), y_2(t), \cdots, y_n(t)\big)^T,$$

and with any different initial values σ, $\tilde{\sigma} \in \mathfrak{F}$, there exists a time point $0 < \tilde{T}(\sigma, \tilde{\sigma}) < +\infty$ called the synchronous ST such that

$$\lim_{t \to \tilde{T}} \|y(t) - x(t)\| = 0, \quad \|y(t) - x(t)\| = 0 \text{ for all } t \geq \tilde{T},$$

and $\tilde{T}(\sigma, \tilde{\sigma}) \leq T$ for all σ, $\tilde{\sigma} \in \mathfrak{F}$. Furthermore, QVNNs (2.1) and (2.2) are said to be PAT synchronized within the preappointed time T_{pat} if

$$\lim_{t \to T_{\text{pat}}} \|y(t) - x(t)\| = 0, \quad \|y(t) - x(t)\| = 0 \text{ for all } t \geq T_{\text{pat}},$$

where $T_{\text{pat}} > 0$ is completely independent of initial values and system parameters.

Definition 2.3 ([32]) The signum function for a quaternion variable $a = a^R + a^I i + a^J j + a^K k \in \mathbb{H}$ is defined as

$$[a] \triangleq \text{sign}(a^R) + \text{sign}(a^I)i + \text{sign}(a^J)j + \text{sign}(a^K)k,$$

where $\text{sign}(a^d)$ is the signum function of a^d, $d = R, I, J, K$.

According to Definition 2.3, for any $a \in \mathbb{H}$, the convex hull of $[a]$ is defined by

$$\overline{\text{co}}\big([a]\big) = \overline{\text{co}}\big[\text{sign}(a^R)\big] + \overline{\text{co}}\big[\text{sign}(a^I)\big]i + \overline{\text{co}}\big[\text{sign}(a^J)\big]j + \overline{\text{co}}\big[\text{sign}(a^K)\big]k,$$

where

$$\overline{\text{co}}\big[\text{sign}(a^d)\big] = \begin{cases} \{1\}, & a^d > 0, \\ [-1, 1], & a^d = 0, \\ \{-1\}, & a^d < 0, \end{cases}$$

and $a^d \in \mathbb{R}$, $d = R, I, J, K$.

Lemma 2.4 For any $a \in \mathbb{H}$ and any measurable selection $\tilde{a} \in \overline{\mathrm{co}}([a])$, the following properties hold:

(1) $\overline{[a]}\tilde{a} + \overline{\tilde{a}}[a] = 2\|[a]\|_1$; (2) $\overline{a}\tilde{a} + \overline{\tilde{a}}a = 2\|a\|_1 \geq 2\|a\|_2$.

Proof When $a^d > 0$, $d = R, I, J, K$, one has that

$$\overline{[a]}\tilde{a} + \overline{\tilde{a}}[a] = 2\overline{(1+i+j+k)}(1+i+j+k) = 8,$$

and similarly, one can prove that

$$\overline{[a]}\tilde{a} + \overline{\tilde{a}}[a] = 8 = 2\|[a]\|_1$$

always holds for $a^d \neq 0$.

For the case where one of a^d is equal to 0, one has that

$$\overline{[a]}\tilde{a} + \overline{\tilde{a}}[a] = 6 = 2\|[a]\|_1.$$

Moreover, when two of a^d are equal to 0, it is easy to get that

$$\overline{[a]}\tilde{a} + \overline{\tilde{a}}[a] = 4 = 2\|[a]\|_1.$$

Furthermore, when three of a^d are equal to 0,

$$\overline{[a]}\tilde{a} + \overline{\tilde{a}}[a] = 2 = 2\|[a]\|_1.$$

In addition, for the case in which $a = 0$,

$$\overline{[a]}\tilde{a} + \overline{\tilde{a}}[a] = 0 = 2\|[a]\|_1.$$

Hence, for any $a \in \mathbb{H}$,

$$\overline{[a]}\tilde{a} + \overline{\tilde{a}}[a] = 2\|[a]\|_1.$$

Similarly, it is easy to derive that

$$\overline{a}\tilde{a} + \overline{\tilde{a}}a = 2(|a^R| + |a^I| + |a^J| + |a^K|) = 2\|a\|_1 \geq 2\|a\|_2.$$

The proof is finished. □

Remark 2.5 The proof method used in Lemma 2.4 is similar to the proof of Lemma 4 in [20]. $\overline{\mathrm{co}}([a])$ in [20] has a total of 9 cases, which are on the complex field. Since the quaternion numbers have two more imaginary parts than the complex numbers, there are 81 cases in $\overline{\mathrm{co}}([a])$ in this paper; this is much more complicated than the proof of Lemma 4 in [20]. In addition, the cases in this paper include the cases in [20]. Therefore, Lemma 4 in [20] can be regarded as a special case of Lemma 2.4 in this paper.

Lemma 2.6 ([32]) For any $a, b \in \mathbb{H}$ and any $e(t) : \mathbb{R} \to \mathbb{H}$, the following properties hold:

(1) $\bar{\bar{a}} = a$; (2) $a + \bar{a} = 2a^R \leq 2\|a\|_2 \leq 2\|a\|_1$; (3) $\overline{ab} = \overline{b}\overline{a}$;

(4) $\frac{\mathrm{d}\|e(t)\|_1}{\mathrm{d}t} = \frac{1}{2}\left([\overline{e(t)}]\frac{\mathrm{d}e(t)}{\mathrm{d}t} + \frac{\mathrm{d}\overline{e(t)}}{\mathrm{d}t}[e(t)]\right)$.

Lemma 2.7 For any $a, b, c \in \mathbb{H}$, the following inequalities hold:

(1) $\left(b^R - |b^I| - |b^J| - |b^K|\right)\|a\|_1 \leq (\overline{[a]}ba)^R \leq \left(b^R + |b^I| + |b^J| + |b^K|\right)\|a\|_1$;

(2) $-\|b\|_1\|c\|_1 \leq (\overline{[a]}bc)^R \leq \|b\|_1\|c\|_1$.

Proof According to the Hamilton criterion,

$$\begin{aligned}(\overline{[a]}ba)^R =& \big(\mathrm{sign}(a^R)b^R + \mathrm{sign}(a^I)b^I + \mathrm{sign}(a^J)b^J + \mathrm{sign}(a^K)b^K\big)\cdot a^R\\ &+ \big(\mathrm{sign}(a^R)b^I - \mathrm{sign}(a^I)b^R - \mathrm{sign}(a^J)b^K + \mathrm{sign}(a^K)b^J\big)\, i\cdot a^I i\\ &+ \big(\mathrm{sign}(a^R)b^J + \mathrm{sign}(a^I)b^K - \mathrm{sign}(a^J)b^R - \mathrm{sign}(a^K)b^I\big)\, j\cdot a^J j\\ &+ \big(\mathrm{sign}(a^R)b^K - \mathrm{sign}(a^I)b^J + \mathrm{sign}(a^J)b^I - \mathrm{sign}(a^K)b^R\big)\, k\cdot a^K k\\ =& |a^R|b^R + \mathrm{sign}(a^I)a^R b^I + \mathrm{sign}(a^J)a^R b^J + \mathrm{sign}(a^K)a^R b^K\\ &- \mathrm{sign}(a^R)a^I b^I + |a^I|b^R + \mathrm{sign}(a^J)a^I b^K - \mathrm{sign}(a^K)a^I b^J\\ &- \mathrm{sign}(a^R)a^J b^J - \mathrm{sign}(a^I)a^J b^K + |a^J|b^R + \mathrm{sign}(a^K)a^J b^I\\ &- \mathrm{sign}(a^R)a^K b^K + \mathrm{sign}(a^I)a^K b^J - \mathrm{sign}(a^J)a^K b^I + |a^K|b^K.\end{aligned}$$

On the one hand,

$$\begin{aligned}(\overline{[a]}ba)^R \le& |a^R|b^R + |a^R||b^I| + |a^R||b^J| + |a^R||b^K|\\ &+ |a^I||b^I| + |a^I|b^R + |a^I||b^K| + |a^I||b^J|\\ &+ |a^J||b^J| + |a^J||b^K| + |a^J|b^R + |a^J||b^I|\\ &+ |a^K||b^K| + |a^K||b^J| + |a^K||b^I| + |a^K|b^K\\ =& \big(b^R + |b^I| + |b^J| + |b^K|\big)|a^R| + \big(b^R + |b^I| + |b^J| + |b^K|\big)|a^I|\\ &\times \big(b^R + |b^I| + |b^J| + |b^K|\big)|a^J| + \big(b^R + |b^I| + |b^J| + |b^K|\big)|a^K|\\ =& \big(b^R + |b^I| + |b^J| + |b^K|\big)\|a\|_1.\end{aligned}$$

On the other hand,

$$\begin{aligned}(\overline{[a]}ba)^R \ge& |a^R|b^R - |a^R||b^I| - |a^R||b^J| - |a^R||b^K|\\ &- |a^I||b^I| + |a^I|b^R - |a^I||b^K| - |a^I||b^J|\\ &- |a^J||b^J| - |a^J||b^K| + |a^J|b^R - |a^J||b^I|\\ &- |a^K||b^K| - |a^K||b^J| - |a^K||b^I| + |a^K|b^K\\ =& \big(b^R - |b^I| - |b^J| - |b^K|\big)|a^R| + \big(b^R - |b^I| - |b^J| - |b^K|\big)|a^I|\\ &+ \big(b^R - |b^I| - |b^J| - |b^K|\big)|a^J| + \big(b^R - |b^I| - |b^J| - |b^K|\big)|a^K|\\ =& \big(b^R - |b^I| - |b^J| - |b^K|\big)\|a\|_1.\end{aligned}$$

According to the above discussion,

$$\big(b^R - |b^I| - |b^J| - |b^K|\big)\|a\|_1 \le (\overline{[a]}ba)^R \le \big(b^R + |b^I| + |b^J| + |b^K|\big)\|a\|_1,$$

which implies that property (1) is true.

Applying a similar method to property (2),

$$\begin{aligned}(\overline{[a]}bc)^R =& \big(\mathrm{sign}(a^R)b^R + \mathrm{sign}(a^I)b^I + \mathrm{sign}(a^J)b^J + \mathrm{sign}(a^K)b^K\big)\cdot c^R\\ &+ \big(\mathrm{sign}(a^R)b^I - \mathrm{sign}(a^I)b^R - \mathrm{sign}(a^J)b^K + \mathrm{sign}(a^K)b^J\big)\, i\cdot c^I i\\ &+ \big(\mathrm{sign}(a^R)b^J + \mathrm{sign}(a^I)b^K - \mathrm{sign}(a^J)b^R - \mathrm{sign}(a^K)b^I\big)\, j\cdot c^J j\\ &+ \big(\mathrm{sign}(a^R)b^K - \mathrm{sign}(a^I)b^J + \mathrm{sign}(a^J)b^I - \mathrm{sign}(a^K)b^R\big)\, k\cdot c^K k\\ =& \mathrm{sign}(a^R)b^R c^R + \mathrm{sign}(a^I)b^I c^R + \mathrm{sign}(a^J)b^J c^R + \mathrm{sign}(a^K)b^K c^R\\ &- \mathrm{sign}(a^R)b^I c^I + \mathrm{sign}(a^I)b^R c^I + \mathrm{sign}(a^J)b^K c^I - \mathrm{sign}(a^K)b^J c^I\end{aligned}$$

$$
\begin{aligned}
&- \operatorname{sign}(a^R)b^Jc^J - \operatorname{sign}(a^I)b^Kc^J + \operatorname{sign}(a^J)b^Rc^J + \operatorname{sign}(a^K)b^Ic^J\\
&- \operatorname{sign}(a^R)b^Kc^K + \operatorname{sign}(a^I)b^Jc^K - \operatorname{sign}(a^J)b^Ic^K + \operatorname{sign}(a^K)b^Kc^K.
\end{aligned}
$$

First,

$$
\begin{aligned}
(\overline{[a]}bc)^R &\le |b^R||c^R| + |b^I||c^R| + |b^J||c^R| + |b^K||c^R| + |b^I||c^I| + |b^R||c^I| + |b^K||c^I| + |b^J||c^I|\\
&\quad + |b^J||c^J| + |b^K||c^J| + |b^R||c^J| + |b^I||c^J|\\
&\quad + |b^K||c^K| + |b^J||c^K| + |b^I||c^K| + |b^K||c^K|\\
&= \big(|b^R| + |b^I| + |b^J| + |b^K|\big)|c^R| + \big(|b^R| + |b^I| + |b^J| + |b^K|\big)|c^I|\\
&\quad \times \big(|b^R| + |b^I| + |b^J| + |b^K|\big)|c^J| + \big(|b^R| + |b^I| + |b^J| + |b^K|\big)|c^K|\\
&= \|b\|_1\|c\|_1.
\end{aligned}
$$

In addition,

$$
\begin{aligned}
(\overline{[a]}bc)^R &\ge - \big(|b^R| + |b^I| + |b^J| + |b^K|\big)|c^R| - \big(|b^R| + |b^I| + |b^J| + |b^K|\big)|c^I|\\
&\quad - \big(|b^R| + |b^I| + |b^J| + |b^K|\big)|c^J| - \big(|b^R| + |b^I| + |b^J| + |b^K|\big)|c^K|\\
&= - \|b\|_1\|c\|_1.
\end{aligned}
$$

Therefore,

$$
-\|b\|_1\|c\|_1 \le (\overline{[a]}bc)^R \le \|b\|_1\|c\|_1.
$$

The proof of Lemma 2.7 is finished. □

Lemma 2.8 ([40]) Assume that there exists a C-regular function $V(e) : \mathbb{R}^n \to \mathbb{R}$ such that

$$
\frac{\mathrm{d}}{\mathrm{d}t}V(e(t)) \le \kappa V(e(t)) - \varphi V^{\theta}(e(t)) - \psi V^{\delta}(e(t)), \quad e(t) \in \mathbb{R}^n \setminus \{0_n\},
$$

where $\kappa \in \mathbb{R}$, $\varphi > 0$, $\psi > 0$, $0 \le \theta < 1$ and $\delta > 1$. Denote that $\varpi = (1-\theta)/(\delta-\theta)$, $\iota = 4\varphi\psi - \kappa^2$. Then

(i) if $\kappa \le 0$, then $V(e(t)) \equiv 0$ and $e(t) \equiv 0$ for $t \ge T_1$, where

$$
T_1 = \frac{\pi}{(\delta-\theta)\varphi}\left(\frac{\varphi}{\psi}\right)^{\varpi}\csc(\varpi\pi);
$$

(ii) if $0 < \kappa < \min\{\varphi, \psi\}$, then $V(e(t)) \equiv 0$ and $e(t) \equiv 0$ for $t \ge T_2$, where

$$
\begin{aligned}
T_2 &= \frac{\pi\csc(\varpi\pi)}{\psi(\delta-\theta)}\left(\frac{\psi}{\varphi-\kappa}\right)^{1-\varpi} I\left(\frac{\psi}{\varphi+\psi-\kappa}, \varpi, 1-\varpi\right)\\
&\quad + \frac{\pi\csc(\varpi\pi)}{\varphi(\delta-\theta)}\left(\frac{\varphi}{\psi-\kappa}\right)^{\varpi} I\left(\frac{\varphi}{\varphi+\psi-\kappa}, 1-\varpi, \varpi\right),
\end{aligned}
$$

and $I(r, p, q)$ is the incomplete Beta function ratio given in [40];

(iii) if $0 < \kappa < 2\sqrt{\varphi\psi}$ and $\delta + \theta = 2$, then $V(e(t)) \equiv 0$ and $e(t) \equiv 0$ for $t \ge T_3$, where

$$
T_3 = \frac{1}{\delta-1}\frac{2}{\sqrt{\iota}}\left(\frac{\pi}{2} + \arctan\left(\frac{\kappa}{\sqrt{\iota}}\right)\right).
$$

Remark 2.9 The lemma cited in [26, 27, 29, 30, 33, 43, 48] requires that

$$
\frac{\mathrm{d}}{\mathrm{d}t}V(e(t)) \le -\varphi V^{\theta}(e(t)) - \psi V^{\delta}(e(t)), \quad e(t) \in \mathbb{R}^n \setminus \{0_n\},
$$

where $\varphi > 0$, $\psi > 0$, $0 \le \theta < 1$ and $\delta > 1$. Obviously, the condition is only a special case of Lemma 2.8. Therefore, Lemma 2.8 introduced in this paper is more general and gives a more accurate estimate of the ST.

Lemma 2.10 ([40]) If there exist a C-regular function $V(e):\mathbb{R}^n\to\mathbb{R}$ and constants κ, $\varphi>0$, $\psi>0$, $0\le\theta<1$, $\delta>1$, $T_{\rm pat}>0$ such that

$$\frac{\mathrm{d}}{\mathrm{d}t}V(e(t))\le-\frac{T}{T_{\rm pat}}\left(-\kappa V(e(t))+\varphi V^{\theta}(e(t))+\psi V^{\delta}(e(t))\right),\quad e(t)\in\mathbb{R}^n\setminus\{0_n\},$$

then $V(e(t))\equiv0$ and $e(t)\equiv0$ for $t\ge T_{\rm pat}$, where

$$T=\begin{cases}T_1, & \kappa\le0,\\ T_2, & 0<\kappa\le\min\{\varphi,\psi\},\\ T_3, & 0<\kappa<2\sqrt{\varphi\psi},\quad \theta+\delta=2.\end{cases}$$

Remark 2.11 Note that the upper bound of convergence time given in Lemma 2.10 is quite different from the counterpart in Lemma 2.9. In fact, the upper estimate T_ϑ in Lemma 2.8 with $\vartheta=1,2,3$ is dependent upon other parameters, but the convergence time $T_{\rm pat}$ in Lemma 2.10 can be prescribed in advance and is unaffected by other parameters.

Lemma 2.12 If $e_p\ge0$, $0<\theta\le1$, $\delta>1$, then

$$\sum_{p=1}^{n}e_p^{\theta}\ge\left(\sum_{p=1}^{n}e_p\right)^{\theta},\quad \sum_{p=1}^{n}e_p^{\delta}\ge n^{1-\delta}\left(\sum_{p=1}^{n}e_p\right)^{\delta}.$$

Assumption 2 For $m=1,2$ and $p\in\vec{n}$, there exist positive real numbers L_p^m, $\tilde{L}_p^m$ and G_p^m such that

$$\|\beta_p-\alpha_p\|_m\le L_p^m\|y_p-x_p\|_m+\tilde{L}_p^m,\qquad \|g_p(\cdot)\|_m\le G_p^m,$$

where $\alpha_p\in\overline{\rm co}[f_p(x_p)]$ and $\beta_p\in\overline{\rm co}[f_p(y_p)]$ with $x_p,y_p\in\mathbb{H}$.

3 Fixed-Time Synchronization

To analyze the FXT synchronization, the following discontinuous controller is designed:

$$u_p(t)=-\left(\mu_p+\varepsilon_p\|e_p(t)\|_1^{\delta}\right)[e_p(t)],\quad p\in\vec{n}.\tag{3.1}$$

Here $\delta>1$ and $\mu_p,\varepsilon_p\in\mathbb{R}$ are positive real constants.

For convenience, denote that

$$k_1=\max_{p\in\vec{n}}\left\{|\xi_p^I|+|\xi_p^J|+|\xi_p^K|-\xi_p^R+L_p^1\sum_{q=1}^{n}\|a_{qp}\|_1\right\},\tag{3.2}$$

$$\varphi_1=\sum_{p=1}^{n}\left(\breve{\mu}-2\sum_{q=1}^{n}G_q^1\|b_{pq}\|_1-\tilde{L}_q^1\sum_{q=1}^{n}\|a_{pq}\|_1\right),\tag{3.3}$$

$$\psi_1=\breve{\varepsilon}n^{1-\delta},\tag{3.4}$$

where $\breve{\mu}=\min\{\mu_p,\ p\in\vec{n}\}$ and $\breve{\varepsilon}=\min\{\varepsilon_p,\ p\in\vec{n}\}$.

Theorem 3.1 Based on Assumptions 1 and 2, under the controller (3.1), if $\varphi_1>0$, then

(1) the master-slave systems (2.1) and (2.2) are FXT synchronized, provided that $k_1\le0$ and the ST is estimated by

$$T(\sigma,\tilde{\sigma})\le\hat{T}_1=\left(\frac{\pi}{\varphi_1\delta}\right)\left(\frac{\varphi_1}{\psi_1}\right)^{\frac{1}{\delta}}\csc\left(\frac{\pi}{\delta}\right);$$

(2) if $0 < k_1 < \min\{\varphi_1, \psi_1\}$, the networks (2.1) and (2.2) are FXT synchronized and the ST is evaluated by

$$T(\sigma,\tilde{\sigma}) \leq \hat{T}_2 = \frac{\pi \csc(\frac{\pi}{\delta})}{\psi_1\delta}\left(\frac{\psi_1}{\varphi_1-k_1}\right)^{1-\frac{1}{\delta}} I\left(\frac{\psi_1}{\varphi_1+\psi_1-k_1}, \frac{1}{\delta}, 1-\frac{1}{\delta}\right) + \frac{\pi \csc(\frac{\pi}{\delta})}{\varphi_1\delta}\left(\frac{\varphi_1}{\psi_1-k_1}\right)^{\frac{1}{\delta}} I\left(\frac{\varphi_1}{\varphi_1+\psi_1-k_1}, 1-\frac{1}{\delta}, \frac{1}{\delta}\right);$$

(3) in particular, when $\delta = 2$ in controller (3.1), the networks (2.1) and (2.2) are FXT synchronized if $0 < k_1 < 2\sqrt{\varphi_1\psi_1}$ and the ST is estimated by

$$T(\sigma,\tilde{\sigma}) \leq \hat{T}_3 = \frac{1}{\delta}\frac{2}{\sqrt{\iota_1}}\left(\frac{\pi}{2} + \arctan\left(\frac{k_1}{\sqrt{\iota_1}}\right)\right),$$

where $\iota_1 = 4\varphi_1\psi_1 - k_1^2 > 0$.

Proof Note that the controller (3.1) is discontinuous, so by the theory of non-smooth analysis [44–46],

$$u_p(t) \in -\left(\mu_p + \varepsilon_p\|e_p(t)\|_1^\delta\right)\overline{\text{co}}([e_p(t)]), \quad p \in \vec{n}.$$

By virtue of the measurable selection theorem [45, 47], a function $\gamma_p(t) \in \overline{\text{co}}([e_p(t)])$ can be found such that

$$u_p(t) = -\left(\mu_p + \varepsilon_p\|e_p(t)\|_1^\delta\right)\gamma_p(t), \quad p \in \vec{n},$$

which, combined with (2.5), gives that

$$\begin{aligned}\frac{\mathrm{d}e_p(t)}{\mathrm{d}t} =& -\xi_p e_p(t) + \sum_{q=1}^n a_{pq}\big(\beta_q(t)-\alpha_q(t)\big) + \sum_{q=1}^n b_{pq}\big(\tilde{\beta}_q(t-\tau_{pq}(t)) - \tilde{\alpha}_q(t-\tau_{pq}(t))\big)\\ &-(\mu_p + \varepsilon_p\|e_p(t)\|_1^\delta)\gamma_p(t), \quad p \in \vec{n}.\end{aligned}$$

Choose the Lyapunov function

$$V_1(e(t)) = \sum_{p=1}^n \|e_p(t)\|_1,$$

where $e(t) = (\|e_1(t)\|_1, \|e_2(t)\|_1, \cdots, \|e_n(t)\|_1)^T \in \mathbb{R}^n$. Calculate the derivative of $V_1(e(t))$ for $e(t) \neq 0$, from Lemma 2.6, one has that

$$\begin{aligned}\frac{\mathrm{d}}{\mathrm{d}t}V_1(e(t)) =& -\frac{1}{2}\sum_{p=1}^n\Big(\overline{[e_p(t)]}\xi_p e_p(t) + \overline{\xi_p e_p(t)}[e_p(t)]\Big)\\ &+\frac{1}{2}\sum_{p=1}^n\sum_{q=1}^n\Big(\overline{[e_p(t)]}a_{pq}\big(\beta_q(t)-\alpha_q(t)\big) + \overline{a_{pq}\big(\beta_q(t)-\alpha_q(t)\big)}[e_p(t)]\Big)\\ &+\frac{1}{2}\sum_{p=1}^n\sum_{q=1}^n\Big(\overline{[e_p(t)]}b_{pq}\big(\tilde{\beta}_q(t-\tau_{pq}(t)) - \tilde{\alpha}_q(t-\tau_{pq}(t))\big)\\ &+\overline{b_{pq}\big(\tilde{\beta}_q(t-\tau_{pq}(t)) - \tilde{\alpha}_q(t-\tau_{pq}(t))\big)}[e_p(t)]\Big)\\ &-\frac{1}{2}\sum_{p=1}^n\Big(\overline{[e_p(t)]}\mu_p\gamma_p(t) + \overline{\mu_p\gamma_p(t)}[e_p(t)]\Big)\\ &-\frac{1}{2}\sum_{p=1}^n\Big(\overline{[e_p(t)]}\varepsilon_p\|e_p(t)\|_1^\delta\gamma_p(t) + \overline{\varepsilon_p\|e_p(t)\|_1^\delta\gamma_p(t)}[e_p(t)]\Big). \qquad (3.5)\end{aligned}$$

Next, we will analyze each term separately in (3.5). By using Lemma 2.6 and Lemma 2.7,

$$-\frac{1}{2}\sum_{p=1}^{n}\Big(\overline{[e_p(t)]}\xi_p e_p(t)+\overline{\xi_p e_p(t)}[e_p(t)]\Big)=-\sum_{p=1}^{n}\Big(\overline{[e_p(t)]}\xi_p e_p(t)\Big)^R$$
$$\leq-\sum_{p=1}^{n}\big(\xi_p^R-|\xi_p^I|-|\xi_p^J|-|\xi_p^K|\big)\,\|e_p(t)\|_1. \tag{3.6}$$

According to Assumption 2, Lemma 2.6 and Lemma 2.7,

$$\begin{aligned}&\frac{1}{2}\sum_{p=1}^{n}\sum_{q=1}^{n}\Big(\overline{[e_p(t)]}a_{pq}\big(\beta_q(t)-\alpha_q(t)\big)+\overline{a_{pq}\big(\beta_q(t)-\alpha_q(t)\big)}[e_p(t)]\Big)\\&=\sum_{p=1}^{n}\sum_{q=1}^{n}\Big(\overline{[e_p(t)]}a_{pq}\big(\beta_q(t)-\alpha_q(t)\big)\Big)^R\leq\sum_{p=1}^{n}\sum_{q=1}^{n}\|a_{pq}\|_1\|\beta_q(t)-\alpha_q(t)\|_1\\&\leq\sum_{p=1}^{n}\sum_{q=1}^{n}\|a_{pq}\|_1\big(L_q^1\|e_q(t)\|_1+\tilde{L}_q^1\big)=\sum_{p=1}^{n}\sum_{q=1}^{n}\big(L_p^1\|a_{qp}\|_1\|e_p(t)\|_1+\tilde{L}_q^1\|a_{pq}\|_1\big).\end{aligned} \tag{3.7}$$

Similarly,

$$\begin{aligned}&\frac{1}{2}\sum_{p=1}^{n}\sum_{q=1}^{n}\Big(\overline{[e_p(t)]}b_{pq}\big(\tilde{\beta}_q(t-\tau_{pq}(t))-\tilde{\alpha}_q(t-\tau_{pq}(t))\big)\\&+\overline{b_{pq}\big(\tilde{\beta}_q(t-\tau_{pq}(t))-\tilde{\alpha}_q(t-\tau_{pq}(t))\big)}[e_p(t)]\Big)\\&\leq\sum_{p=1}^{n}\sum_{q=1}^{n}\|b_{pq}\|_1\|\tilde{\beta}_q(t-\tau_{pq}(t))-\tilde{\alpha}_q(t-\tau_{pq}(t))\|_1\leq 2\sum_{p=1}^{n}\sum_{q=1}^{n}\|b_{pq}\|_1G_q^1.\end{aligned} \tag{3.8}$$

Moreover, based on Lemma 2.4,

$$-\frac{1}{2}\sum_{p=1}^{n}\Big(\overline{[e_p(t)]}\mu_p\gamma_p(t)+\overline{\mu_p\gamma_p(t)}[e_p(t)]\Big)=-\sum_{p=1}^{n}\mu_p\|[e_p(t)]\|_1,$$

and

$$-\frac{1}{2}\sum_{p=1}^{n}\Big(\overline{[e_p(t)]}\varepsilon_p\|e_p(t)\|_1^\delta\gamma_p(t)+\overline{\varepsilon_p\|e_p(t)\|_1^\delta\gamma_p(t)}[e_p(t)]\Big)=-\sum_{p=1}^{n}\varepsilon_p\|[e_p(t)]\|_1\|e_p(t)\|_1^\delta. \tag{3.9}$$

Plugging (3.6)–(3.9) into (3.5), and from Lemma 2.12, for $e(t)\neq 0$,

$$\begin{aligned}\frac{\mathrm{d}}{\mathrm{d}t}V_1(e(t))\leq&\sum_{p=1}^{n}\Big(|\xi_p^I|+|\xi_p^J|+|\xi_p^K|-\xi_p^R+L_p^1\sum_{q=1}^{n}\|a_{qp}\|_1\Big)\|e_p(t)\|_1\\&-\sum_{p=1}^{n}\Big(\mu_p\|[e_p(t)]\|_1-2\sum_{q=1}^{n}G_q^1\|b_{pq}\|_1-\sum_{q=1}^{n}\tilde{L}_q^1\|a_{pq}\|_1\Big)\\&-\sum_{p=1}^{n}\varepsilon_p\|[e_p(t)]\|_1\|e_p(t)\|_1^\delta\\\leq& k_1\sum_{p=1}^{n}\|e_p(t)\|_1-\sum_{p=1}^{n}\Big(\check{\mu}-2\sum_{q=1}^{n}G_q^1\|b_{pq}\|_1-\sum_{q=1}^{n}\tilde{L}_q^1\|a_{pq}\|_1\Big)\\&-\check{\varepsilon}n^{1-\delta}\Big(\sum_{p=1}^{n}||e_p(t)||_1\Big)^\delta\\=& k_1V_1(e(t))-\varphi_1-\psi_1V_1^\delta(e(t)).\end{aligned} \tag{3.10}$$

If $k_1 \leq 0$, for $e(t) \in \mathbb{R}^n \setminus \{0_n\}$,

$$\frac{\mathrm{d}}{\mathrm{d}t}V_1(e(t)) \leq -\varphi_1 - \psi_1 V_1^{\delta}(e(t)), \tag{3.11}$$

which, with Lemma 2.8 (i), gives that the networks (2.1) and (2.2) are FXT synchronized within the time $\hat{T}_1$. Similarly, the remaining results in Theorem 3.1 can be easily obtained from Lemma 2.8 (ii) and (iii). □

Theorem 3.1 is presented under 1-norm; in fact, the FXT synchronization can also be ensured under 2-norm.

The controller is designed as

$$u_p(t) = -\left(\mu_p + \varepsilon_p \|e_p(t)\|_2^{\delta}\right)[e_p(t)], \quad p \in \vec{n}, \tag{3.12}$$

where $\delta > 1$, $\mu_p, \varepsilon_p \in \mathbb{R}$ are positive real constants.

Denote that

$$k_2 = \max_{p\in\vec{n}}\left\{\frac{1}{2}\sum_{q=1}^{n}\left(\|a_{qp}\|_2 L_p^2 + \|a_{pq}\|_2 L_q^2\right) - \xi_p^R\right\}, \tag{3.13}$$

$$\varphi_2 = \min_{p\in\vec{n}}\left\{-\sum_{q=1}^{n}\left(2G_q^2\|b_{pq}\|_2 + \tilde{L}_q^2\|a_{pq}\|_2\right) + \mu_p\right\}, \tag{3.14}$$

$$\psi_2 = \check{\varepsilon} n^{\frac{1-\delta}{2}}, \tag{3.15}$$

where $\check{\varepsilon} = \min\{\varepsilon_p,\ p \in \vec{n}\}$.

Theorem 3.2 Based on Assumptions 1 and 2, under the controller (3.12), if $\varphi_2 > 0$, then

(1) the networks (2.1) and (2.2) are FXT synchronized provided that $k_2 \leq 0$ and that the ST is estimated by

$$T(\sigma,\tilde{\sigma}) \leq \check{T}_1 = \left(\frac{2\pi}{\varphi_2\delta}\right)\left(\frac{\varphi_2}{\psi_2}\right)^{\frac{1}{\delta}}\csc\left(\frac{\pi}{\delta}\right);$$

(2) if $0 < k_2 < \min\{\varphi_2, \psi_2\}$, the networks (2.1) and (2.2) are FXT synchronized and the ST is evaluated by

$$\begin{aligned} T(\sigma,\tilde{\sigma}) \leq \check{T}_2 = {} & \frac{2\pi\csc(\frac{\pi}{\delta})}{\psi_2\delta}\left(\frac{\psi_2}{\varphi_2 - k_2}\right)^{1-\frac{1}{\delta}} I\left(\frac{\psi_2}{\varphi_2+\psi_2-k_2}, \frac{1}{\delta}, 1-\frac{1}{\delta}\right) \\ & + \frac{2\pi\csc(\frac{\pi}{\delta})}{\varphi_2\delta}\left(\frac{\varphi_2}{\varphi_2 - k_2}\right)^{\frac{1}{\delta}} I\left(\frac{\varphi_2}{\varphi_2+\psi_2-k_2}, 1-\frac{1}{\delta}, \frac{1}{\delta}\right); \end{aligned}$$

(3) in particular, when $\delta = 2$ in controller (3.12), the networks (2.1) and (2.2) are FXT synchronized if $0 < k_2 < 2\sqrt{\varphi_2\psi_2}$ and the ST is estimated by

$$T(\sigma,\tilde{\sigma}) \leq \check{T}_3 = \frac{2}{\delta-1}\frac{2}{\sqrt{\iota_2}}\left(\frac{\pi}{2} + \arctan\left(\frac{k_2}{\sqrt{\iota_2}}\right)\right),$$

where $\iota_2 = 4\varphi_2\psi_2 - k_2^2 > 0$.

Proof Similarly, a function $\gamma_p(t) \in \overline{\mathrm{co}}([e_p(t)])$ can be selected such that

$$\begin{aligned} \frac{\mathrm{d}e_p(t)}{\mathrm{d}t} = {} & -\xi_p e_p(t) + \sum_{q=1}^{n} a_{pq}\big(\beta_q(t) - \alpha_q(t)\big) + \sum_{q=1}^{n} b_{pq}\big(\tilde{\beta}_q(t-\tau_{pq}(t)) - \tilde{\alpha}_q(t-\tau_{pq}(t))\big) \\ & - (\mu_p + \varepsilon_p\|e_p(t)\|_2^{\delta})\gamma_p(t), \quad p \in \vec{n}. \end{aligned}$$

Choose the Lyapunov function $V_2(e(t)) = \frac{1}{2}\sum\limits_{p=1}^{n}\|e_p(t)\|_2^2$, where $e(t) = \big(\|e_1(t)\|_2^2, \|e_2(t)\|_2^2, \cdots, \|e_n(t)\|_2^2\big)^T \in \mathbb{R}^n$. From the error system, when $e(t) \neq 0$, one has that

$$\begin{aligned}\frac{\mathrm{d}}{\mathrm{d}t}V_2(e(t)) =& -\frac{1}{2}\sum_{p=1}^{n}\Big(\xi_p e_p(t)\overline{e_p(t)} + e_p(t)\overline{\xi_p e_p(t)}\Big)\\ &+\frac{1}{2}\sum_{p=1}^{n}\sum_{q=1}^{n}\Big(a_{pq}\big(\beta_q(t)-\alpha_q(t)\big)\overline{e_p(t)} + e_p(t)\overline{a_{pq}\big(\beta_q(t)-\alpha_q(t)\big)}\Big)\\ &+\frac{1}{2}\sum_{p=1}^{n}\sum_{q=1}^{n}\Big(b_{pq}\big(\tilde{\beta}_q(t-\tau_{pq}(t))-\tilde{\alpha}_q(t-\tau_{pq}(t))\big)\overline{e_p(t)}\\ &+e_p(t)\overline{b_{pq}\big(\tilde{\beta}_q(t-\tau_{pq}(t))-\tilde{\alpha}_q(t-\tau_{pq}(t))\big)}\Big)\\ &-\frac{1}{2}\sum_{p=1}^{n}\big(\mu_p\gamma_p(t)\overline{e_p(t)} + e_p(t)\overline{\mu_p\gamma_p(t)}\big)\\ &-\frac{1}{2}\sum_{p=1}^{n}\big(\varepsilon_p\gamma_p(t)\|e_p(t)\|_2^{\delta}\overline{e_p(t)} + e_p(t)\overline{\varepsilon_p\gamma_p(t)\|e_p(t)\|_2^{\delta}}\big). \end{aligned} \tag{3.16}$$

According to Lemma 2.6,

$$\begin{aligned}-\frac{1}{2}\sum_{p=1}^{n}\Big(\xi_p e_p(t)\overline{e_p(t)} + e_p(t)\overline{\xi_p e_p(t)}\Big) &= -\frac{1}{2}\sum_{p=1}^{n}\big(\xi_p\|e_p(t)\|_2^2 + e_p(t)\overline{e_p(t)\xi_p}\big)\\ &= -\frac{1}{2}\sum_{p=1}^{n}(\xi_p+\overline{\xi_p})\|e_p(t)\|_2^2 = -\sum_{p=1}^{n}\xi_p^R\|e_p(t)\|_2^2. \end{aligned} \tag{3.17}$$

Moreover,

$$\begin{aligned}&\frac{1}{2}\sum_{p=1}^{n}\sum_{q=1}^{n}\Big(a_{pq}\big(\beta_q(t)-\alpha_q(t)\big)\overline{e_p(t)} + e_p(t)\overline{a_{pq}\big(\beta_q(t)-\alpha_q(t)\big)}\Big)\\ \le& \sum_{p=1}^{n}\sum_{q=1}^{n}\|a_{pq}(\beta_q(t)-\alpha_q(t))e_p(t)\|_2\\ \le& \sum_{p=1}^{n}\sum_{q=1}^{n}\big(\|a_{pq}\|_2 L_q^2\|e_q(t)\|_2\|e_p(t)\|_2 + \tilde{L}_q^2\|a_{pq}\|_2\|e_p(t)\|_2\big)\\ \le& \frac{1}{2}\sum_{p=1}^{n}\sum_{q=1}^{n}(\|a_{qp}\|_2 L_p^2 + \|a_{pq}\|_2 L_q^2)\|e_p(t)\|_2^2 + \sum_{p=1}^{n}\sum_{q=1}^{n}\tilde{L}_q^2\|a_{pq}\|_2\|e_p(t)\|_2. \end{aligned}$$

Similarly,

$$\begin{aligned}&\frac{1}{2}\sum_{p=1}^{n}\sum_{q=1}^{n}\Big(b_{pq}\big(\tilde{\beta}_q(t-\tau_{pq}(t))-\tilde{\alpha}_q(t-\tau_{pq}(t))\big)\overline{e_p(t)}\\ &+e_p(t)\overline{b_{pq}\big(\tilde{\beta}_q(t-\tau_{pq}(t))-\tilde{\alpha}_q(t-\tau_{pq}(t))\big)}\Big)\\ \le& \sum_{p=1}^{n}\sum_{q=1}^{n}\|b_{pq}(\tilde{\beta}_q(t-\tau_{pq}(t))-\tilde{\alpha}_q(t-\tau_{pq}(t)))e_p(t)\|_2\\ \le& 2\sum_{p=1}^{n}\sum_{q=1}^{n}\|b_{pq}\|_2 G_q^2\|e_p(t)\|_2. \end{aligned} \tag{3.18}$$

Moreover, from Lemma 2.4,

$$-\frac{1}{2}\sum_{p=1}^{n}\left(\mu_p\gamma_p(t)\overline{e_p(t)}+e_p(t)\overline{\mu_p\gamma_p(t)}\right)\leq-\sum_{p=1}^{n}\mu_p\|e_p(t)\|_2, \tag{3.19}$$

$$-\frac{1}{2}\sum_{p=1}^{n}\left(\varepsilon_p\gamma_p(t)\|e_p(t)\|_2^{\delta}\overline{e_p(t)}+e_p(t)\overline{\varepsilon_p\gamma_p(t)\|e_p(t)\|_2^{\delta}}\right)\leq-\sum_{p=1}^{n}\varepsilon_p\|e_p(t)\|_2^{\delta+1}. \tag{3.20}$$

According to (3.17)–(3.19),

$$\begin{aligned}\frac{\mathrm{d}}{\mathrm{d}t}V_2(e(t))&\leq\sum_{p=1}^{n}\left[\sum_{q=1}^{n}\frac{1}{2}\left(\|a_{qp}\|_2L_p^2+\|a_{pq}\|_2L_q^2\right)-\xi_p^R\right]\|e_p(t)\|_2^2\\&\quad-\sum_{p=1}^{n}\left(\mu_p-2\sum_{q=1}^{n}G_q^2\|b_{pq}\|_2-\sum_{q=1}^{n}\tilde{L}_q^2\|a_{pq}\|_2\right)\|e_p(t)\|_2-\sum_{p=1}^{n}\varepsilon_p\|e_p(t)\|_2^{\delta+1}\\&=k_2V_2(e(t))-\varphi_2V_2^{\frac{1}{2}}(e(t))-\psi_2V_2^{\frac{\delta+1}{2}}(e(t)).\end{aligned} \tag{3.21}$$

Therefore, it is easy to get, based on Lemma 2.8, that the networks (2.1) and (2.2) are FXT synchronized. □

Remark 3.3 Compared with previous studies on the FXT synchronization of QVNNs using the separation method [26–30], it is clear that the non-separated direct method used in this paper can significantly reduce computational redundancy. At the same time, by virtue of introducing a quaternion sign function, the 1-norm and the 2-norm, the quaternion controllers (3.1) and (3.12) are designed directly in this paper, this is a method that is more concise and efficient than adding four real-valued controllers as in [26–30].

Remark 3.4 The authors in [33] only introduced the 1-norm to analyze the FNT synchronization of QVNNs with and without delay. In this paper, the FXT synchronization of QVNNs is explored based on 1-norm and the quadratic norm. More specifically, Theorem 3.1 is established by applying the 1-norm to construct Lyapunov function and to design the controller, but Theorem 3.2 is obtained by introducing the quadratic norm. Note that the two results, including synchronization criteria and the estimates for the synchronization time, are totally different. Hence, our results are more plentiful and flexible compared with related work that is only based on a single type of norm.

Remark 3.5 In [48], the authors discussed the problem of FXT consensus for a class of heterogeneous nonlinear multiagent systems based on the result of fixed-time stability given in [18]. As opposed to that work, the FXT synchronization of QVNNs is investigated based on the improved theorem of fixed-time stability [19]. It has been revealed that the estimate for the settling time provided in [19] is more accurate compared with that of [18], which indirectly improves the estimation accuracy of synchronization in our paper.

4 Preassigned-Time Synchronization

The PAT synchronization of QVNNs (2.1) and (2.2) will be analyzed below. To achieve this, the following control strategies are proposed:

$$u_p(t)=-\frac{\hat{T}_1}{T_{\mathrm{pat}}}\left(\mu_p+\varepsilon_p\|e_p(t)\|_1^{\delta}\right)[e_p(t)],\quad p\in\vec{n}, \tag{4.1}$$

$$u_p(t) = -\frac{\hat{T}_2}{T_{\rm pat}}\left(\mu_p + \varepsilon_p\|e_p(t)\|_1^{\delta}\right)[e_p(t)], \quad p \in \vec{n}, \tag{4.2}$$

$$u_p(t) = -\frac{\hat{T}_3}{T_{\rm pat}}\left(\mu_p + \varepsilon_p\|e_p(t)\|_1^{2}\right)[e_p(t)], \quad p \in \vec{n}. \tag{4.3}$$

Here $\delta > 1$, $\mu_p > 0$, $\varepsilon_p > 0$, $T_{\rm pat} > 0$ is a preassigned time, and $\hat{T}_\vartheta$ is defined as in Theorem 3.1 with $\vartheta = 1, 2, 3$.

Theorem 4.1 Under Assumptions 1 and 2, the following PAT synchronization results are established:

(1) if $k_1 \le 0$, the networks (2.1) and (2.2) are PAT synchronized within the preassigned time $T_{\rm pat}$ satisfying that $0 < T_{\rm pat} \le \hat{T}_1$ under the control law (4.1);

(2) if $0 < k_1 < \min\{\varphi_1, \psi_1\}$, the networks (2.1) and (2.2) are PAT synchronized within the preassigned time $T_{\rm pat}$ satisfying that $0 < T_{\rm pat} \le \hat{T}_2$ under the control law (4.2);

(3) if $0 < k_1 < 2\sqrt{\varphi_1\psi_1}$, the networks (2.1) and (2.2) are PAT synchronized within the preassigned time $T_{\rm pat}$ satisfying that $0 < T_{\rm pat} \le \hat{T}_3$ under the control strategy (4.3).

Proof This is similar to the proof of Theorem 3.1. Note that $0 < T_{\rm pat} \le \hat{T}_1$ and $k_1 \le 0$, so when $e(t) \ne 0$,

$$\begin{aligned}\frac{\rm d}{{\rm d}t}V_1(e(t)) &\le -\sum_{p=1}^{n}\sum_{q=1}^{n}\left(\frac{\hat{T}_1}{T_{\rm pat}}\check{\mu} - G_q^1\|b_{pq}\|_1 - \tilde{L}_q^1\|a_{pq}\|_1\right) - \sum_{p=1}^{n}\frac{\hat{T}_1}{T_{\rm pat}}\check{\varepsilon}n^{1-\delta}V_1^{\delta}(e(t))\\ &\le -\frac{\hat{T}_1}{T_{\rm pat}}\left(\varphi_1 + \psi_1 V_1^{\delta}(e(t))\right).\end{aligned}$$

According to Lemma 2.8, QVNNs (2.1) and (2.2) are PAT synchronized within the time $T_{\rm pat}$.

For the case where $0 < k_1 < \min\{\varphi_1, \psi_1\}$, it is easy to obtain that

$$\frac{\rm d}{{\rm d}t}V_1(e(t)) \le k_1 V_1(e(t)) - \frac{\hat{T}_2}{T_{\rm pat}}\varphi_1 - \frac{\hat{T}_2}{T_{\rm pat}}\psi_1 V_1^{\delta}(e(t)).$$

Therefore, when $e(t) \ne 0$,

$$\frac{\rm d}{{\rm d}t}V_1(e(t)) \le -\frac{\hat{T}_2}{T_{\rm pat}}\left(-k_1 V_1(e(t)) + \varphi_1 + \psi_1 V_1^{\delta}(e(t))\right),$$

which implies that QVNNs (2.1) and (2.2) achieve PAT synchronization within the time $T_{\rm pat}$.

For the case where $0 < k_1 < 2\sqrt{\varphi_1\psi_1}$, the proof is similar to the above analysis, so is omitted here. □

Next, the following control strategies based on 2-norm are proposed in order to realize PAT synchronization of networks (2.1) and (2.2):

$$u_p(t) = -\frac{\check{T}_1}{T_{\rm pat}}\left(\mu_p + \varepsilon_p\|e_p(t)\|_2^{\delta}\right)[e_p(t)], \quad p \in \vec{n}, \tag{4.4}$$

$$u_p(t) = -\frac{\check{T}_2}{T_{\rm pat}}\left(\mu_p + \varepsilon_p\|e_p(t)\|_2^{\delta}\right)[e_p(t)], \quad p \in \vec{n}, \tag{4.5}$$

$$u_p(t) = -\frac{\check{T}_3}{T_{\rm pat}}\left(\mu_p + \varepsilon_p||e_p(t)||_2^{2}\right)[e_p(t)], \quad p \in \vec{n}. \tag{4.6}$$

Here $\delta > 1$, $\mu_p > 0$, $\varepsilon_p > 0$, $T_{\rm pat} > 0$ is a preassigned time, and $\check{T}_\vartheta$ is defined as in Theorem 3.2 with $\vartheta = 1, 2, 3$.

Theorem 4.2 Under Assumptions 1 and 2, the following PAT synchronization results are established:

(1) If $k_2 \leq 0$, the networks (2.1) and (2.2) are PAT synchronized within the preassigned time $T_{\rm pat}$, satisfying that $0 < T_{\rm pat} \leq \check{T}_1$ under the control law (4.4);

(2) if $0 < k_2 < \min\{\varphi_2, \psi_2\}$, the networks (2.1) and (2.2) are PAT synchronized within the preassigned time $T_{\rm pat}$, satisfying that $0 < T_{\rm pat} \leq \check{T}_2$ under the control strategy (4.5);

(3) if $0 < k_2 < 2\sqrt{\varphi_2\psi_2}$, the networks (2.1) and (2.2) are PAT synchronized within the preassigned time $T_{\rm pat}$, satisfying that $0 < T_{\rm pat} \leq \check{T}_3$ under the controller (4.6).

Remark 4.3 If the preassigned synchronized time is $T_{\rm pat} > \hat{T}_\vartheta$ $(\vartheta = 1, 2, 3)$ as in Theorem 4.1, it follows from Theorem 3.1 that the PAT synchronization can be also achieved under the controller (3.1), since the synchronization has been realized within the time $\hat{T}_\vartheta$. Similarly, if the preassigned synchronized time is $T_{\rm pat} > \check{T}_\vartheta$ $(\vartheta = 1, 2, 3)$ as in Theorem 4.2, it follows from Theorem 3.2 that the PAT synchronization can be also achieved under the controller (3.12).

Remark 4.4 Recently, much has been published on the synchronization of QVNNs, including on global synchronization [13, 14], exponential synchronization [15, 16], quasi synchronization [50, 51], FNT anti-synchronization [32], FXT synchronization [26, 27, 29, 30, 33]. However, there are few results on the PAT synchronization of QVNNs. In [28], the PAT synchronization of QVNNs without delay was analyzed based on four real-valued controllers by a separation method. In Theorems 4.1 and 4.2 in this paper, we have studied PAT synchronization of QVNNs with a time-varying delay by designing quaternion controllers based on the unseparated method. It is evident that the quaternion controllers designed in this paper is simpler.

Remark 4.5 Note that the synchronization can be also solved for a specified time in advance under the FXT control schemes (3.1) and (3.12) by adjusting the control parameters. However, the adjustment may be seriously troublesome, since the relation between the convergence time and the parameters are not clear. Moreover, the quicker convergence time may result in larger control costs. To avoid these shortcomings, the control protocols (4.1)–(4.6) have been developed in order to achieve the preassigned-time synchronization.

5 Numerical Examples

In this section, some numerical examples are presented in order to verify the correctness of the above theoretical results.

Example 5.1 Consider the QVNN

$$\dot{x}(t) = -\xi x(t) + \mathfrak{A}f(x(t)) + \mathfrak{B}g(x(t-\tau(t))) + \mathfrak{I}, \tag{5.1}$$

where $x(t) = (x_1(t), x_2(t))^T$, and the activation functions are given by

$$f(x(t)) = \begin{pmatrix} f_1^R(x_1^R(t)) + if_1^I(x_1^I(t)) + jf_1^J(x_1^J(t)) + kf_1^K(x_1^K(t)) \\ f_2^R(x_2^R(t)) + if_2^I(x_2^I(t)) + jf_2^J(x_2^J(t)) + kf_2^K(x_2^K(t)) \end{pmatrix}$$

and

$$g(x(t)) = \begin{pmatrix} g_1^R(x_1^R(t)) + ig_1^I(x_1^I(t)) + jg_1^J(x_1^J(t)) + kg_1^K(x_1^K(t)) \\ g_2^R(x_2^R(t)) + ig_2^I(x_2^I(t)) + jg_2^J(x_2^J(t)) + kg_2^K(x_2^K(t)) \end{pmatrix},$$

where $f_q^d(x_q^d(t)) = \sin(x_q^d(t)) + 0.01\text{sign}(x_q^d(t))$ and $g_q^d(x_q^d(t)) = \big(|x_q^d(t)+1| - |x_q^d(t)-1|\big)/2$, $q = 1, 2$. Obviously, $L_q^1 = 1$, $\tilde{L}_q^1 = 0.02$ and $G_q^1 = 4$. The time-varying delay is $\tau(t) = e^t/\big(1+e^t\big)$. In addition,

$$\xi = \text{diag}(\xi_1, \xi_2) = \begin{pmatrix} 0.6 + 0.5i - 0.4j - 0.1k & 0 \\ 0 & 0.2 + 0.1i - 0.5j - 0.5k \end{pmatrix},$$

$$\mathfrak{A} = (a_{pq})_{2\times 2} = \begin{pmatrix} -0.4 + 0.8i - 0.2j + 0.6k & 0.1 - 0.4i - 0.4j - 0.8k \\ 0.1 + 0.6i + 0.7j - 0.5k & 0.3 + 0.4i - 0.2j + 1.0k \end{pmatrix},$$

$$\mathfrak{B} = (b_{pq})_{2\times 2} = \begin{pmatrix} 0.2 - 0.5i - 0.7j - 0.1k & 0.5 + 0.4i - 0.2j - 0.3k \\ -0.2 + 0.5i - 0.3j - 0.1k & 0.4 - 0.4i - 0.4j + 0.5k \end{pmatrix},$$

$$\mathfrak{I} = (I_p)_{2\times 1} = \begin{pmatrix} -2.0 + 1.0i + 1.2j - 2.5k \\ 1.5 + 0.4i - 1.8j + 0.6k \end{pmatrix}.$$

The dynamic behavior of system (5.1) is presented in Figure 1.

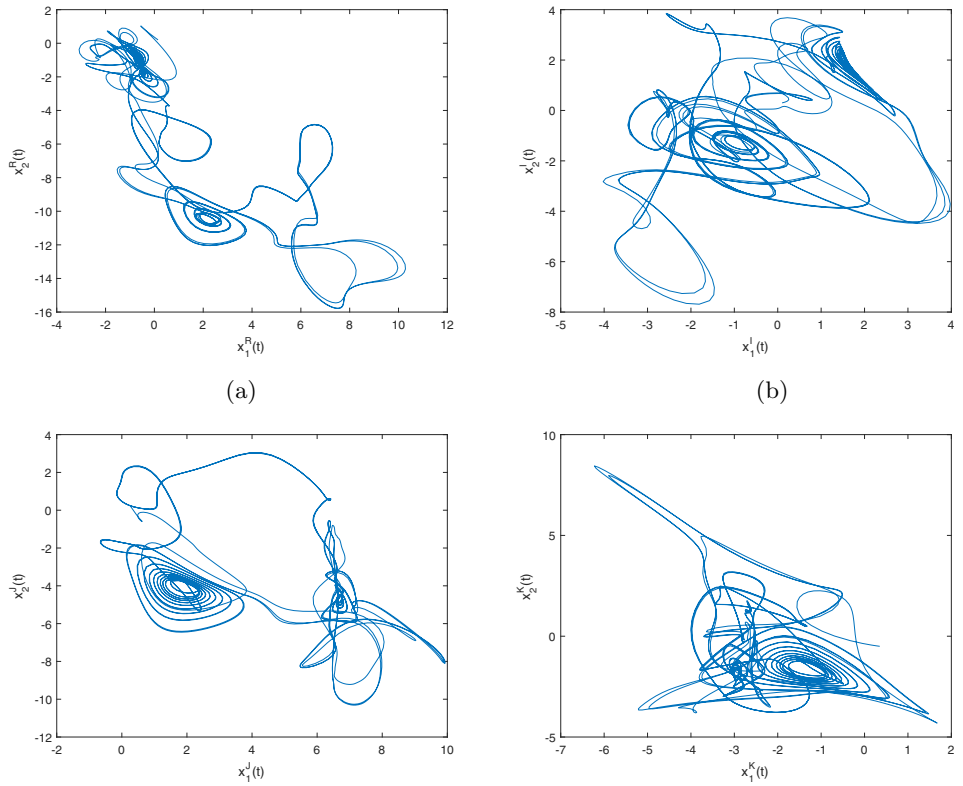

Figure 1 Dynamic behavior of system (5.1)

The response system is described by

$$\dot{y}(t) = -\xi y(t) + \mathfrak{A} f(y(t)) + \mathfrak{B} g(y(t-\tau(t))) + \mathfrak{I} + \mathfrak{U}(t), \tag{5.2}$$

where $y(t) = (y_1(t), y_2(t))^T$, $\mathfrak{U}(t) = (u_1(t), u_2(t))^T$ is the controller, which will be shown later.

First, the FXT synchronization of networks (5.1) and (5.2) will be verified. Consider the controller designed in Theorem 3.1:

$$u_p(t) = -\left(\mu_p + \varepsilon_p \|e_p(t)\|_1^{\delta}\right)[e_p(t)], \quad p \in \{1, 2\}. \tag{5.3}$$

By a simple calculation, we get that $k_1 = 4.90$. Select $\mu_1 = 25.5$, $\mu_2 = 25.5$, $\varepsilon_1 = 7.5$, $\varepsilon_2 = 7.5$ and $\delta = 1.5$. It is evident that, $\breve{\mu} = 25.5$ and $\breve{\varepsilon} = 7.5$. Therefore, $\varphi_1 = 5.25$, $\psi_1 = 5.30$, and the inequality $0 < k_1 < \min\{\varphi_1, \psi_1\}$ is satisfied. According to Theorem 3.1, the FXT synchronization is ensured and the ST is estimated by $T_1 = 3.1215$. The simulation result is presented in Figure 2 by picking random initial values.

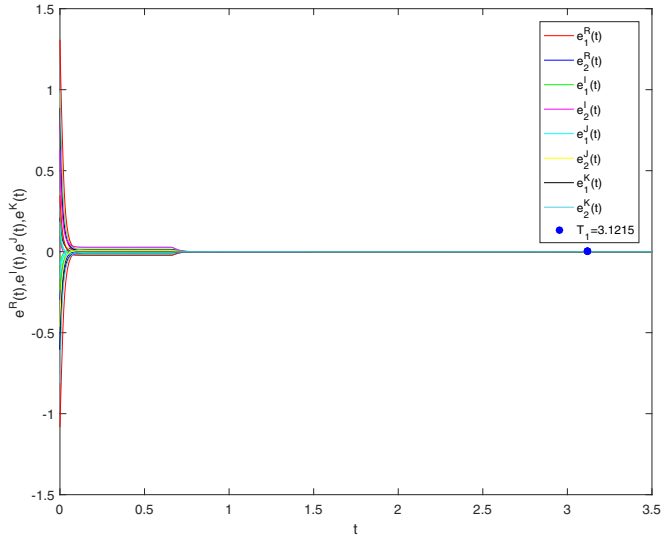

Figure 2 FXT synchronization of master-slave systems (5.1) and (5.2)

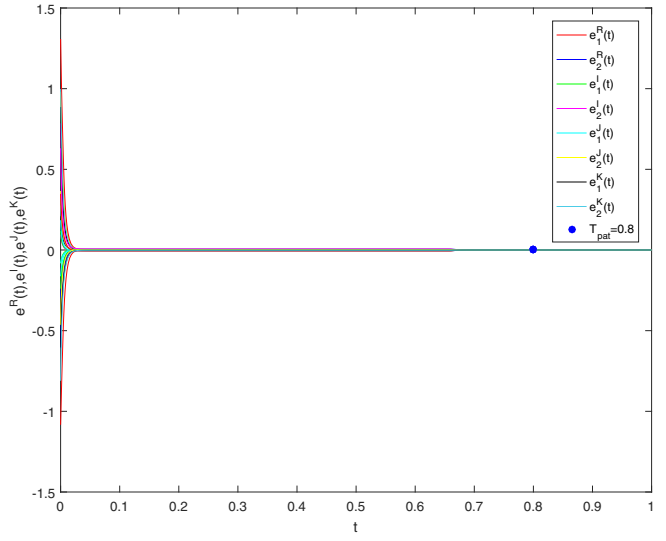

Figure 3 PAT synchronization of master-slave systems (5.1) and (5.2)

In what follows, the PAT synchronization of networks (5.1) and (5.2) will be verified. Selecting $T_{\rm pat}=0.8$, the control scheme is given as

$$u_p(t)=-\frac{T_1}{T_{\rm pat}}\left(\mu_p+\varepsilon_p\|e_p(t)\|_1^{\delta}\right)[e_p(t)],\quad p\in\{1,2\},\tag{5.4}$$

in which $\mu_1=25.5$, $\mu_2=25.5$, $\varepsilon_1=7.5$, $\varepsilon_2=7.5$ and $\delta=1.5$. According to Theorem 4.1, systems (5.1) and (5.2) are PAT synchronized within the preassigned time $T_{\rm pat}=0.8$. The corresponding numerical result is illustrated in Figure 3, by picking random initial values.

Next, the FXT synchronization and the PAT synchronization under 2-norm will be verified in Example 5.2, according to Theorem 3.2 and Theorem 4.2.

Example 5.2 Consider the QVNN

$$\dot{x}(t)=-\xi x(t)+\mathfrak{A}f(x(t))+\mathfrak{B}g(x(t-\tau(t)))+\mathfrak{I},\tag{5.5}$$

where $x(t)=(x_1(t),x_2(t))^T$, and the activation functions are

$$f(x(t)=\begin{pmatrix}f_1^R(x_1^R(t))+if_1^I(x_1^I(t))+jf_1^J(x_1^J(t))+kf_1^K(x_1^K(t))\\ f_2^R(x_2^R(t))+if_2^I(x_2^I(t))+jf_2^J(x_2^J(t))+kf_2^K(x_2^K(t))\end{pmatrix}$$

and

$$g(x(t)=\begin{pmatrix}g_1^R(x_1^R(t))+ig_1^I(x_1^I(t))+jg_1^J(x_1^J(t))+kg_1^K(x_1^K(t))\\ g_2^R(x_2^R(t))+ig_2^I(x_2^I(t))+jg_2^J(x_2^J(t))+kg_2^K(x_2^K(t))\end{pmatrix},$$

where $f_q^d(x_q^d(t))=\tanh(x_q^d(t))$ and $g_q^d(x_q^d(t))=\big(|x_q^d(t)+1|-|x_q^d(t)-1|\big)/2$, $q=1,2$. Obviously, $L_q^2=1$, $\tilde{L}_q^2=0$ and $G_q^2=2$. The time-varying delay is $\tau(t)=e^t/\big(1+e^t\big)$. In addition,

$$\xi=\mathrm{diag}(\xi_1,\xi_2)=\begin{pmatrix}-0.04-0.10i+6.80j+3.10k & 0\\ 0 & 0.02+0.01i-1.50j-2.00k\end{pmatrix},$$

$$\mathfrak{A}=(a_{pq})_{2\times2}=\begin{pmatrix}0.6+0.5i+0.5j-0.6k & -0.3+0.1i-0.1j+0.4k\\ 0.2+0.6i-0.2j+0.5k & 0.1+0.2i+0.3j-0.6k\end{pmatrix},$$

$$\mathfrak{B}=(b_{pq})_{2\times2}=\begin{pmatrix}0.6+0.9i+0.1j+0.1k & -0.6+0.4i-0.1j+0.6k\\ -0.1-0.7i+0.2j-0.4k & 0.5-0.3i+0.4j+0.2k\end{pmatrix},$$

$$\mathfrak{I}=(I_p)_{2\times1}=\begin{pmatrix}-0.1-0.1i-1.2j+1.3k\\ 0.5+1.4i-1.8j+0.6k\end{pmatrix}.$$

The dynamic behavior of system (5.5) is presented in Figure 4.

The response system is described by

$$\dot{y}(t)=-\xi y(t)+\mathfrak{A}f(y(t))+\mathfrak{B}g(y(t-\tau(t)))+\mathfrak{I}+\mathfrak{U}(t),\tag{5.6}$$

where $y(t)=(y_1(t),y_2(t))^T$, $\mathfrak{U}(t)=(u_1(t),u_2(t))^T$ is the controller, which will be shown later.

First, the FXT synchronization will be verified. Consider the control strategy designed in Theorem 3.2:

$$u_p(t)=-\left(\mu_p+\varepsilon_p\|e_p(t)\|_2^{\delta}\right)[e_p(t)],\quad p\in\{1,2\}.\tag{5.7}$$

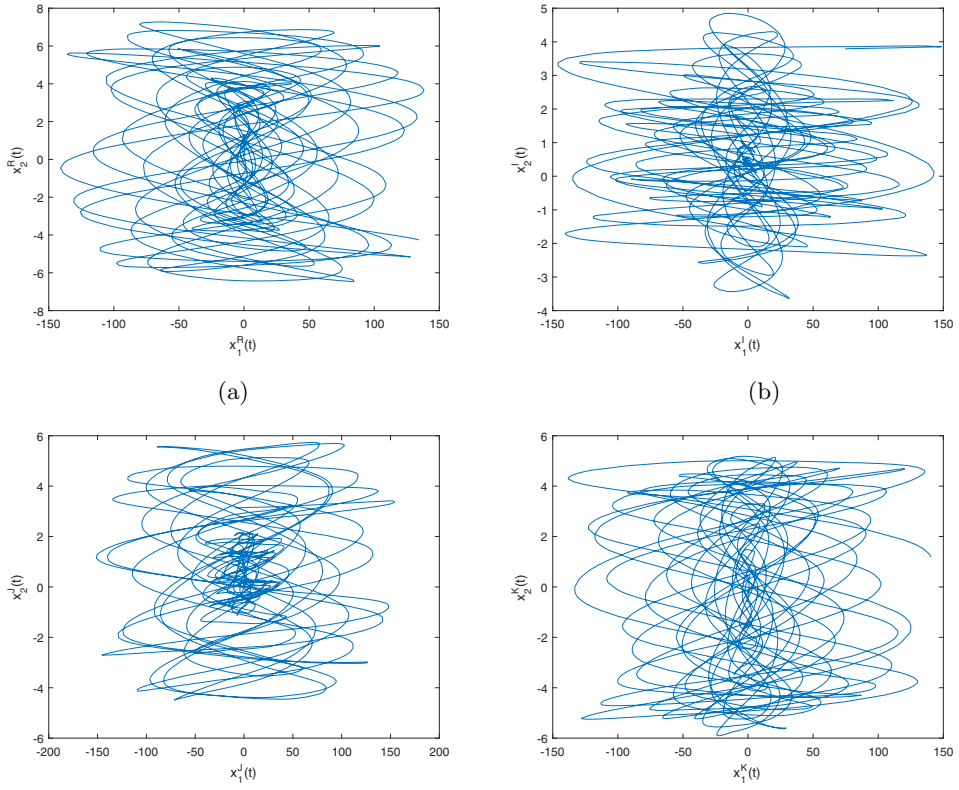

(a) (b)

(c) (d)

Figure 4 Dynamic behavior of system (5.5)

By a simple calculation, $k_2 = 1.7835$, $\varphi_2 = 1$ and $\psi_2 = 2.1213$. Select $\mu_1 = 9.1371$, $\mu_2 = 7.2860$, $\varepsilon_1 = 3$, $\varepsilon_2 = 5$ and $\delta = 2$. Then, $k_2 < 2\sqrt{\varphi_2\psi_2} = 5.8259$. According to Theorem 3.2, the FXT synchronization is realized within the time $T_2 = 3.8726$. The simulation result is presented in Figure 5 by picking random initial values.

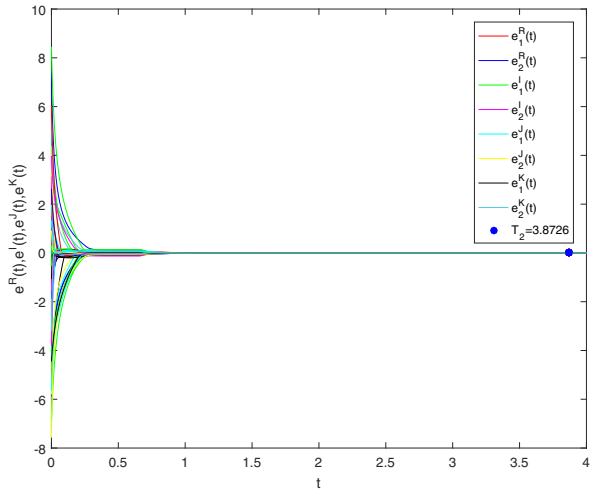

Figure 5 FXT synchronization of master-slave systems (5.5) and (5.6)

In what follows, the PAT synchronization of networks (5.5) and (5.6) will be verified. Selecting $T_{\rm pat} = 0.8$, the control scheme is given as

$$u_p(t) = -\frac{T_2}{T_{\rm pat}} \left(\mu_p + \varepsilon_p \|e_p(t)\|_2^{\delta}\right) [e_p(t)], \quad p \in \{1, 2\}, \tag{5.8}$$

in which $\mu_1 = 9.1371$, $\mu_2 = 7.2860$, $\varepsilon_1 = 3$, $\varepsilon_2 = 5$ and $\delta = 2$. From Theorem 4.2, systems (5.5) and (5.6) are PAT synchronized within the preassigned time $T_{\rm pat} = 0.8$. The corresponding numerical result is illustrated in Figure 6 by picking random initial values.

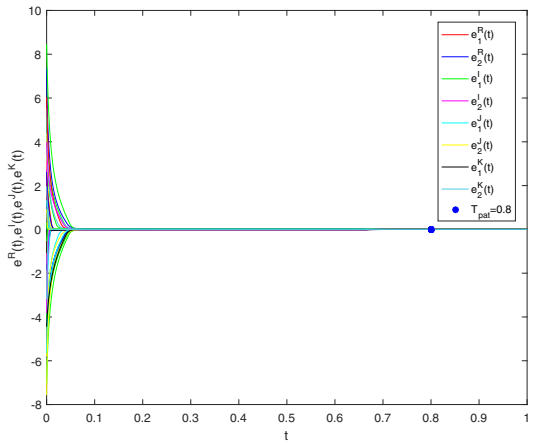

Figure 6 PAT synchronization of master-slave systems (5.5) and (5.6)

6 Conclusion

In this article, the FXT synchronization and the PAT synchronization for a class of QVNNs with time-varying delay and discontinuous activation functions were achieved by designing a direct quaternion controller based on a non-separation method. Compared with the existing results [26–31, 33, 34], our results have the advantage of less computation, a simpler control design, lower conservatism and more accurate estimation of ST. It is noted that stochastic disturbance and the switching effect are inevitable in neural circuits and practical problems [52, 53], so it would be valuable and meaningful to investigate the FXT and PAT synchronization of QVNNs; this will be one of the directions of our future research.

References

[1] Shuai J, Chen Z, Liu R, Wu B. The Hamilton neural network model recognition of the color patterns. Chinese Journal of Computers, 1995, **5**: 372–379

[2] Took C, Mandic D. The quaternion LMS algorithm for adaptive filtering of hypercomplex processes. IEEE Transactions on Signal Processing, 2009, **57**: 1316–1327

[3] Zou C, Kou K, Wang Y. Quaternion collaborative and sparse representation with application to color face recognition. IEEE Transactions on Image Processing, 2016, **25**: 3287–3302

[4] Liu Y, Zheng Y, Lu J, et al. Constrained quaternion-variable convex optimization: A quaternion-valued recurrent neural network approach. IEEE Transactions on Neural Networks and Learning Systems, 2019, **31**: 1022–1035

[5] Liu Y, Zhang D, Lu J, Cao J. Global μ-stability criteria for quaternion-valued neural networks with unbounded time-varying delays. Information Sciences, 2016, **360**: 273–288

[6] You X, Song Q, Liang J, et al. Global μ-stability of quaternion-valued neural networks with mixed time-varying delays. Neurocomputing, 2018, **290**: 12–25
[7] Shu H, Song Q, Liu Y, et al. Global μ-stability of quaternion-valued neural networks with non-differentiable time-varying delays. Neurocomputing, 2017, **247**: 202–212
[8] Li L, Chen W. Exponential stability analysis of quaternion-valued neural networks with proportional delays and linear threshold neurons: Continuous-time and discrete-time cases. Neurocomputing, 2020, **381**: 152–166
[9] Qi X, Bao H, Cao J. Exponential input-to-state stability of quaternion-valued neural networks with time delay. Applied Mathematics and Computation, 2019, **358**: 382–393
[10] Xu X, Xu Q, Yang J, et al. Further research on exponential stability for quaternion-valued neural networks with mixed delays. Neurocomputing, 2020, **400**: 186–205
[11] Pratap A, Raja R, Cao J, et al. $O(t^{-\beta})$-Synchronization and asymptotic synchronization of delayed fractional order neural networks. Acta Mathematica Scientia, 2022, **42B**(4): 1273–1292
[12] Li R, Wu H, Cao J. Impulsive exponential synchronization of fractional-order complex dynamical networks with derivative couplings via feedback control based on discrete time state observations. Acta Mathematica Scientia, 2022, **42B**(2): 737–754
[13] Li H, Jiang H, Cao J. Global synchronization of fractional-order quaternion-valued neural networks with leakage and discrete delays. Neurocomputing, 2019, **385**: 211–219
[14] Xiao J, Zhong S. Synchronization and stability of delayed fractional-order memristive quaternion-valued neural networks with parameter uncertainties. Neurocomputing, 2019, **363**: 321–338
[15] Chen Y, Zhang X, Xue Y. Global exponential synchronization of high-order quaternion Hopfield neural networks with unbounded distributed delays and time-varying discrete delays. Mathematics and Computers in Simulation, 2022, **193**: 173–189
[16] Lin D, Chen X, Yu G, et al. Global exponential synchronization via nonlinear feedback control for delayed inertial memristor-based quaternion-valued neural networks with impulses. Applied Mathematics and Computation, 2021, **401**: 126093
[17] Li H, Hu C, Zhang L, et al. Non-separation method-based robust finite-time synchronization of uncertain fractional-order quaternion-valued neural networks. Applied Mathematics and Computation, 2021, **409**: 126377
[18] Polyakov A. Nonlinear feedback design for fixed-time stabilization of linear control systems. IEEE Transactions on Automatic Control, 2012, **57**: 2106–2110
[19] Hu C, Yu J, Chen Z, et al. Fixed-time stability of dynamical systems and fixed-time synchronization of coupled discontinuous neural networks. Neural Networks, 2017, **89**: 74–83
[20] Feng L, Yu J, Hu C, et al. Nonseparation method-based finite/fixed-time synchronization of fully complex-valued discontinuous neural networks. IEEE Transactions on Cybernetics, 2021, **51**: 3212–3223
[21] Zhang Y, Zhuang J, Xia Y, et al. Fixed-time synchronization of the impulsive memristor-based neural networks. Communications in Nonlinear Science and Numerical Simulation, 2019, **77**: 40–53
[22] Li H, Li C, Huang T, Zhang W. Fixed-time stabilization of impulsive Cohen-Grossberg BAM neural networks. Neural Networks, 2018, **98**: 203–211
[23] Xiao J, Zeng Z, Wen S, et al. Finite-/Fixed-time synchronization of delayed coupled discontinuous neural networks with unified control schemes. IEEE Transactions on Neural Networks and Learning Systems, 2021, **32**: 2535–2546
[24] Feng L, Hu C, Yu J, et al. Fixed-time synchronization of coupled memristive complex-valued neural networks. Chaos, Solitons and Fractals, 2021, **148**: 110993
[25] Xiong K, Yu J, Hu C, Jiang H. Synchronization in finite/fixed time of fully complex-valued dynamical networks via nonseparation approach. Journal of the Franklin Institute, 2020, **357**: 473–493
[26] Deng H, Bao H. Fixed-time synchronization of quaternion-valued neural networks. Physica A: Statistical Mechanics and Its Applications, 2019, **527**: 121351
[27] Kumar U, Das S, Huang C, Cao J. Fixed-time synchronization of quaternion-valued neural networks with time-varying delay. Proceedings of the Royal Society A: Mathematical, Physical and Engineering Sciences, 2020, **476**: 20200324
[28] Wei W, Yu J, Wang L, et al. Fixed/Preassigned-time synchronization of quaternion-valued neural networks via pure power-law control. Neural Networks, 2022, **146**: 341–349
[29] Wei R, Cao J. Fixed-time synchronization of quaternion-valued memristive neural networks with time

delays. Neural Networks, 2019, **113**: 1–10
[30] Chen D, Zhang W, Cao J, Huang C. Fixed time synchronization of delayed quaternion-valued memristor-based neural networks. Advances in Diffffference Equations, 2020, **2020**: 92–108
[31] Song X, Man J, Song S, Ahn C. Finite/Fixed-time anti-synchronization of inconsistent Markovian quaternion-valued memristive neural networks with reaction-diffusion terms. IEEE Transactions on Circuits and Systems I: Regular Papers, 2021, **68**: 363–375
[32] Li Z, Liu X. Finite time anti-synchronization of quaternion-valued neural networks with asynchronous time-varying delays. Neural Processing Letters, 2020, **52**: 2253–2274
[33] Peng T, Qiu J, Lu J, et al. Finite-time and fixed-time synchronization of quaternion-valued neural networks with/without mixed delays: An improved one-norm method. IEEE Transactions on Neural Networks and Learning Systems, 2021, **99**: 1–13
[34] Peng T, Zhong J, Tu Z, et al. Finite-time synchronization of quaternion-valued neural networks with delays: A switching control method without decomposition. Neural Networks, 2022, **148**: 37–47
[35] Forti M, Nistri P. Global convergence of neural networks with discontinuous neuron activations. IEEE Transactions on Circuits and Systems I: Fundamental Theory and Applications, 2003, **50**: 1421–1435
[36] Forti M, Grazzini M, Nistri P. Generalized Lyapunov approach for convergence of neural networks with discontinuous or nonlipschitz activations. Physica D, 2006, **214**: 88–99
[37] Hu C, Jiang H. Special functions-based fixed-time estimation and stabilization for dynamic systems. IEEE Transactions on Systems, Man, and Cybernetics: Systems, 2022, **52**: 3251–3262
[38] Zhang Y, Guo J, Xiang Z. Finite-time adaptive neural control for a class of nonlinear systems with asymmetric time-varying full-state constraints. IEEE Transactions on Neural Networks and Learning Systems, 2022. DOI:10.1109/TNNLS.2022.3164948
[39] Cui D, Xiang Z. Nonsingular fixed-time fault-tolerant fuzzy control for switched uncertain nonlinear systems. IEEE Transactions on Fuzzy Systems, 2022. DOI:10.1109/TFUZZ.2022.3184048
[40] Hu C, He H, Jiang H. Fixed/Preassigned-time synchronization of complex networks via improving fixed-time stability. IEEE Transactions on Cybernetics, 2021, **51**: 2882–2892
[41] Liu X, Ho D, Xie C. Prespecified-time cluster synchronization of complex networks via a smooth control approach. IEEE Transactions on Cybernetics, 2020, **50**: 1771–1775
[42] Shao S, Liu X, Cao J. Prespecified-time synchronization of switched coupled neural networks via smooth controllers. Neural Networks, 2021, **133**: 32–39
[43] Liu X, Chen T. Finite-time and fixed-time cluster synchronization with or without pinning control. IEEE Transactions on Cybernetics, 2018, **48**: 240–252
[44] Clarke F. Optimization and Nonsmooth Analysis. New York: Wiley, 1983
[45] Filippov A F. Differential equations with discontinuous right-hand side. Amer Math Soc Trans, 1964,**42**: 199–231
[46] Huang L, Guo Z, Wang J. Theory and Applications of Differential Equations with Discontinuous Right-Hand Sides. Beijing: Science Press, 2011
[47] Aubin J, Frankowska H. Set-Valued Analysis. Boston: Birkhäuser, 1990
[48] Zou W, Qian K, Xiang Z. Fixed-time consensus for a class of heterogeneous nonlinear multiagent systems. IEEE Transactions on Circuits and Systems-II: Express Briefs, 2020, **67**: 1279–1283
[49] Liu X, Chen T. Global exponential stability for complex-valued recurrent neural networks with asynchronous time delays. IEEE Transactions on Neural Networks and Learning Systems, 2016, **27**: 593–606
[50] Li R, Gao X, Cao J. Quasi-state estimation and quasi-synchronization control of quaternion-valued fractional-order fuzzy memristive neural networks: Vector ordering approach. Applied Mathematics and Computation, 2019, **362**: 124572
[51] Li R, Cao J, Xue C, Manivannan R. Quasi-stability and quasi-synchronization control of quaternion-valued fractional-order discrete-time memristive neural networks. Applied Mathematics and Computation, 2021, **395**: 125851
[52] Anand K, Yogambigai J, Harish Babu G, et al. Synchronization of singular Markovian jumping neutral complex dynamical networks with time-varying delays via pinning control. Acta Mathematica Scientia, 2020, **40B**(3): 863–886
[53] Rajasekar S, Pitchaimani M, Zhu Q. Probing a stochastic epidemic hepatitis C virus model with a chronically infected treated population. Acta Mathematica Scientia, 2022, **42B**(5): 2087–2112